Single pulse excimer laser nanostructuring of thin silicon films: Nanosharp cones formation and a heat transfer problem

Julia Eizenkop,[a] Ivan Avrutsky, and Gregory Auner[b]
Department of Electrical and Computer Engineering, Wayne State University, Detroit, Michigan 48202

Daniel G. Georgiev
Department of Electrical Engineering and Computer Science, University of Toledo, Toledo, Ohio 43606-3390

Vipin Chaudhary
Department of Computer Science and Engineering, The State University of New York, Buffalo, New York 14260

(Received 6 December 2006; accepted 23 December 2007; published online 3 May 2007)

We present analytical and computer modeling along with an experiment on the formation of sharp conical tips on monocrystalline silicon thin films, silicon-on-insulator, subjected to irradiation by single 25 ns pulses from a KrF excimer laser focused into a spot several micrometers in diameter. These fabricated structures have heights of about 1 μm and apical radii of curvature of several tens of nanometers. We offer a simplified analytical model for the formation of these structures. The computer simulation includes two-dimensional time-dependant heat transfer and phase transformations in Si films on SiO_2 substrates that result from the laser irradiation (the Stefan problem). It is shown that upon irradiation and initial melting, the liquid/solid interface remains mainly parallel to the surface of the film. After the laser pulse, the molten material self-cools and resolidifies. The solid/liquid interface moves predominately laterally toward the center of the irradiated spot, forming an almost vertical front. We discuss the relation between the dynamics of the melting/freezing front movement and the displacement of material in the irradiated spot. © *2007 American Institute of Physics*. [DOI: 10.1063/1.2720185]

I. INTRODUCTION

Reliable, simple, and low-cost techniques for fabrication of micro- and nanotips of silicon and other semiconductor and metal materials, as well as large, high-density arrays of such tips, are desirable in a number of technological applications. These include probes for scanning probe microscopy techniques, emitters for field-emission-based devices such as high-definition displays,[1] and other vacuum microelectronics applications.[2] There is also a growing amount of research on surface patterning of materials for biomedical applications,[3–5] which could also benefit from new developments in the area of materials surface micro- and nanostructuring.

Remarkable Si columns with heights of about 20 μm and widths of $2-3$ μm have been produced by multiple-pulse, large-spot, nanosecond excimer laser irradiation (KrF laser, $\lambda=248$ nm) of Si wafers in oxygen and oxygen-containing ambient.[6] Conditions for nanostructuring of Si surfaces have been identified in a study of the irradiation of bulk Si as a function of the number and the fluence of the applied KrF excimer laser pulses in different gas environments.[7] The below-band gap absorbance of femtosecond-laser microstructured silicon holds great promise for application in silicon based optoelectronics.[8] Femtosecond laser ablation of chalcogenide glass leads to the formation of nanofibers with a very high length to diameter ratio.[9] Formation of nanobumps was observed on silicon irradiated by KrF laser through polystyrene[10] or silica[11] microspheres.

The technique that is of interest to this study is based on a single-pulse excimer-laser irradiation that allows one to controllably fabricate Si tips (and dense arrays of such tips) with heights in the range of $0.2-2$ μm and with an apical radius of curvature of several tens of nanometers. Conditions for controllable, direct laser fabrication of sharp conical structures on silicon thin films have been previously published[12] and the first results on field emission properties of these nanosharp cones have been reported recently.[13] Hereafter, these sharp conical tips are referred to as nanotips. The laser radiation is absorbed entirely in a thin surface layer (the absorption coefficient of Si at $\lambda=248$ nm is about 1.8×10^6 cm^{-1}). This surface layer becomes a source of heat that causes melting of the entire thickness of the film: under the conditions of irradiation, the depth of melting of bulk silicon would be more than the thickness of the film.[14] Because the underlying silica has a much lower thermal conductivity than Si, heat is dissipated predominantly in a lateral direction through the surrounding Si film volume.

II. EXPERIMENT

Spatially homogenized, single pulses of radiation from a KrF excimer laser ($\lambda=248$ nm, Lambda Physik, model LPX 205) were used to image pinholes or slits onto uniformly illuminated circular spots or lines on the sample surface by

[a]Electronic mail: juliaei@comcast.net
[b]Electronic mail: ag0770@wayne.edu

 © 2007 American Institute of Physics

Downloaded 21 Oct 2008 to 128.205.254.133. Redistribution subject to AIP license or copyright; see http://jap.aip.org/jap/copyright.jsp

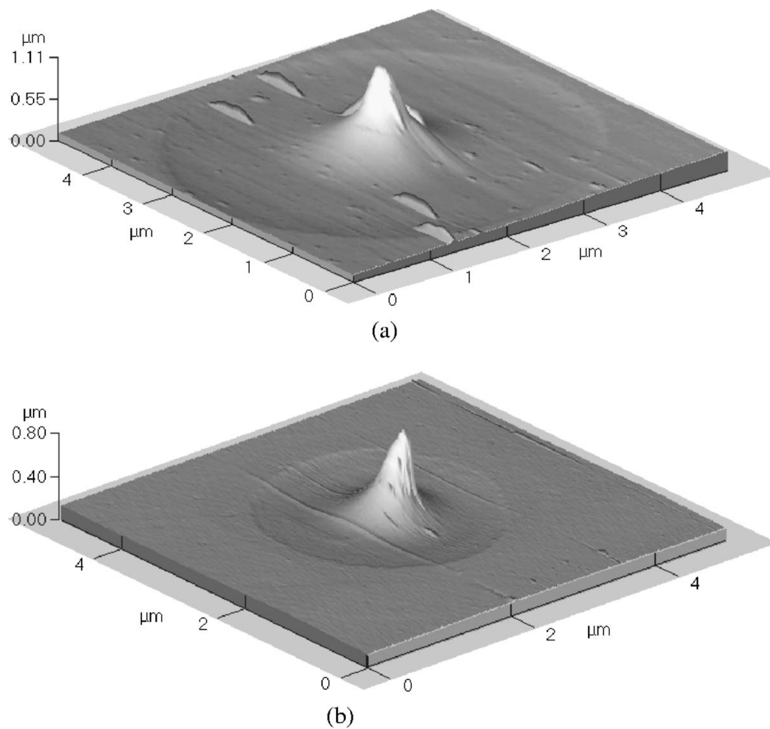

FIG. 1. AFM images of a nanotips fabricated by a single pulse with fluence of 1.5 J/cm^2 and laser spots with radiuses (a) 2.8 and (b) 1.7 μm.

means of a projection system with a demagnification factor of 8.9 and a resolution limit of 2 μm. The laser pulse energy was measured to be stable within 5%. Most of the work was done on commercially acquired silicon-on-insulator (SOI) wafers that consisted of 200 nm (100) single-crystal Si bonded to a silica glass substrate. The atomic force microscopy (AFM) images of tips fabricated by a single pulse of fluence 1.5 J/cm^2 on 200 nm thick Si film are shown on Fig. 1. In addition, SOI wafers that consisted of a single-crystal Si layer on 1 μm layer of silica on a bulk Si substrate were used. These were plasma-etch-thinned to different thicknesses of the Si layer in the range of 0.8–4.1 μm. The laser processing was performed in ambient, clean-room conditions, and the sample surface topography was then examined by contact-mode atomic force microscopy on a Park Autoprobe LS AFM system using Contact Ultralever® tips.

III. ANALYTICAL MODEL

Building a comprehensive model of the nanotips formation is a difficult task because there is a combination of complex physical and chemical processes that are responsible for the results of nanosecond-pulse, high-energy irradiation of thin films.

Apparently, irradiation by a nanosecond laser pulse causes a mass transfer in the film, bringing material from the edges of the irradiated spot to its center. It is clear, however, that the very starting point in the analysis of any possible mechanism of the tip formation is the heat transfer problem. It has been indicated previously that the geometry of the thin-film structure and of the laser spot may lead to predominantly lateral heat dissipation.[15] The shape of melting/solidification fronts and their propagation mode within the irradiated film is critical for further understanding of this mass transfer. In particular, because liquid silicon is denser than silicon in its solid state, the liquid tends to move in the direction that the melting/solidification front moves. Such a mechanism was first proposed in Ref. 16 as a possible explanation of how the micron-scale periodical heating pattern generates relief gratings in laser annealing of germanium. Remarkably, the groves profiles predicted by a simplified model[17] are qualitatively very similar to the profiles of the nanotips and nanoridges fabricated by laser annealing of silicon films.[18] The mechanism of lateral motion of molted silicon associated with different densities of liquid and solid material was also studied in a recent article.[19] Another possible mechanism that was used to explain a sharp profile on bulk silicon subjected to a single pulse, shaped to a spot several microns in diameter, relies on thermocapillary forces associated with temperature gradients in the melt.[20] In both cases evolution of the temperature distribution in the irradiated spot defines the motion of liquid material.

We have verified experimentally that in our case the irradiation of bulk Si wafers under conditions identical to those applied to the thin film samples (single pulses with fluences in the range of 0.8–3.0 J/cm^2, and the several micron spot size) produced no observable changes on the bulk wafer surface. Therefore, in our case limiting the dissipation of heat from the laser-heated spot to predominantly lateral (two-dimensional) transfer within the Si film during resolidification was a critical condition. Another important factor is that Si has higher density (ρ=2.52 g/cm^3) in its liquid state than in its solid state (ρ=2.33 g/cm^3 for crystalline Si and ρ=2.2 g/cm^3 for amorphous Si).

Our analytical model is actually a simplified model of mass transfer. During the lateral resolidification (that starts on the perimeter of the melted spot) every infinitesimal layer (with a fixed mass) will expand to a greater volume. The layer can expand only toward the center and upward, pushing the rest of liquid silicon toward the center and upward

Downloaded 21 Oct 2008 to 128.205.254.133. Redistribution subject to AIP license or copyright; see http://jap.aip.org/jap/copyright.jsp

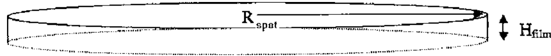

FIG. 2. Irradiated spot with radius R that is much bigger than film thickness.

and forming a cone. To assure the predominantly lateral heat transfer we need the condition $R_{spot} > (\sigma\tau)^{1/2} > H_{film}$ be satisfied, where σ is thermal diffusivity, τ is the duration of the laser pulse, R_{spot} is the laser spot radius, and H_{film} is the thickness of silicon film (see Fig. 2). In our experiment $\sqrt{\sigma\tau} \approx 0.7$ μm at the end of the pulse. Since fused silica is not an ideal thermal insulator, for predominantly lateral heat flow we also need a condition $Q_{lat} > Q_{substr}$ to be satisfied, where Q_{lat} and Q_{substr} are the radial heat flow along the film and the vertical heat flow into the substrate, respectively. Since

$$Q_{lat} \approx 2\pi R_{spot} H_{film} k_{Si} \overline{\partial T/\partial r}|_{r=R_0},$$

(k is the thermal conductivity) and

$$Q_{subst} \approx \pi (R_{spot})^2 k_{Si} \overline{\partial T/\partial z}|_{z=z_b},$$

where $\overline{\partial T/\partial z}$ is a vertical gradient averaged over the radius and $\overline{\partial T/\partial r}$ is a radial gradient averaged over the z values. It leads to

$$R_{spot} < (2H_{film}\overline{\partial T/\partial r}|_{r=R_0})/\overline{\partial T/\partial z}|_{z=z_b},$$

where z_b is a z coordinate of Si/SiO_2 interface.

We can combine the two conditions into one lateral heat flow criterion

$$H_{film} < \sqrt{\sigma\tau} \leq R_{spot} < (2H_{film}\overline{\partial T/\partial r}|_{r=R_0})/(\overline{\partial T/\partial z}|_{z=z_b}). \quad (1)$$

Because of the difference in liquid/solid densities the wafer surface is above the liquid spot surface. For simplicity we assume below that the liquid surface is flat. Since the heat transfer is predominantly lateral, at the time of solidification the liquid/solid interface moves toward the center of irradiated spot and the interface will become almost vertical. This interface is represented by the conical surface showed in Fig. 3(a) and defined by the cross-section AOO_1A_1. Figure 3(b) illustrates how the cross-section changes when the radius of melt decreases by value dR. The melted Si is located between two circles of radii R and $r=R-H\tan\beta=A_1O_1$. Since the thickness of the film is less than a thermal diffusion length at the end of the pulse, it is reasonable to assume that the temperature near the Si/SiO_2 (point O_1) is only slightly lower than the temperature on the Si surface (point O) and

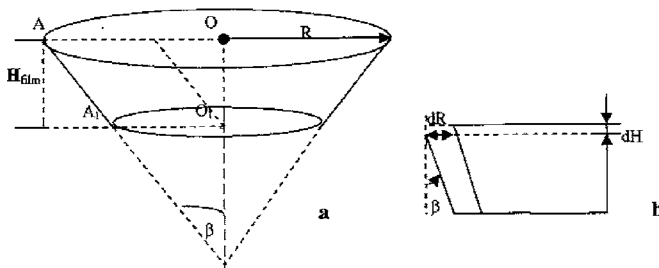

FIG. 3. (a) The melt is restricted by a part of the conical surface with a cross-section AOO_1A_1 and (b) small changes in cross-section AOO_1A_1.

the angle β between the isothermal surface and the vertical line is small. Below, subscripts L and S denote liquid and solid states accordingly. By using $V_{cone}=1/3\pi R^2 H$ and upon implementing an appropriate algebraic transformation one can obtain

$$V_L = \pi R^2 H - \pi R H^2 \tan\beta + \pi H^3 (\tan\beta)^2/3 \quad (2)$$

for the volume of the melt. From this equation we have the differential change of melt volume dV_L with change in radius dR,

$$\begin{aligned} dV_L(R) &= V_L(R+dR) - V(R) \\ &= \pi H dR(2R - H\tan\beta) \\ &= -dV_S(R) \times (R+dR). \end{aligned} \quad (3)$$

The density of solid Si is lower than that of liquid Si and therefore the resolidified Si occupies a larger volume than melted Si. Thus the solid/liquid interface, which is moving toward the center, pushes the surface level of the remaining liquid Si upwards. Therefore we can write the change of melt volume as $dV_L(dH)=\pi R^2 dH$. The mass conservation equation for this process (in first order by dR and dH) is given by

$$(\rho_L - \rho_S)\pi H dR(2R - H\tan\beta) + \rho_L \pi R^2 dH = 0. \quad (4a)$$

Hence,

$$dH/dR = -(\rho_L - \rho_S)/\rho_L(2R - H\tan\beta)H/R^2. \quad (4b)$$

Let us designate $(\rho_L - \rho_S)/\rho_L = \mu$ (equals 0.08 for liquid and monocrystalline Si) and $y=H/R$. Then we obtain $dH/dR = y + R dy/dR$ and Eq. (4b) transforms to

$$\frac{dy}{y[1+\mu(2-y\times\tan\beta)]} = -\frac{dR}{R}. \quad (5)$$

After integrating Eq. (5) it is not difficult to obtain the expression

$$\frac{H}{H_o}\left[1 - \frac{H\mu\times\tan\beta}{(1+2\mu)R}\right] = \left(\frac{R_o}{R}\right)^{2\mu}. \quad (6)$$

In Eq. (6), H_o is the initial height of the liquid layer and R_o is the irradiated spot radius. This equation is valid until the distance A_1O_1 becomes equal to zero [Fig. 3(a)]. At this point, one obtains $R=R_{cr}=H_{cr}\tan\beta$ and the solidification process is almost complete. Substituting $R=R_{cr}$ in Eq. (6) one obtains the expression for H_{cr},

$$H_{cr} = R_o\left[\frac{H_o(1+2\mu)}{R_o(1+\mu)(\tan\beta)^{2\mu}}\right]^{1/(2\mu+1)}. \quad (7)$$

Within the scope of this model (β=const), for $R<R_{cr}$ the remaining liquid can only move up. One obtains a height of $H(R)=H_{cr}+(R_{cr}-R)\mu/\tan\beta$ which yields a maximum height of

$$H(0) = H_{cr}(1+\mu). \quad (8)$$

Solving Eq. (5) against H one can obtain the dependence for $H(R)$,

Downloaded 21 Oct 2008 to 128.205.254.133. Redistribution subject to AIP license or copyright; see http://jap.aip.org/jap/copyright.jsp

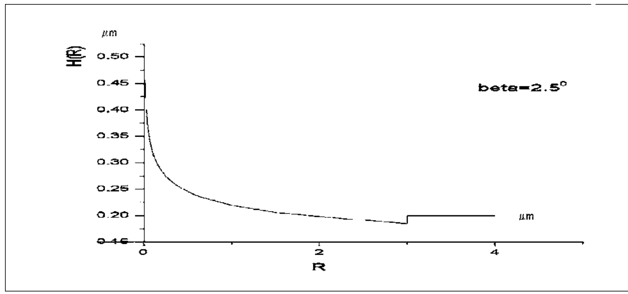

FIG. 4. Conical structure according to formula (9) for β=2.5°.

$$H = \frac{H_o[1-\sqrt{1-2A(R_o/R)^{2\mu+1}}]}{AR_o/R} \quad \text{where } A = \frac{2\mu \tan \beta H_o}{(1+2\mu)R_o}. \tag{9}$$

The dependence $H(R)$ according to Eq. (9) with β =2.5° is shown in Fig. 4.

We assume that fast ultraviolet laser resolidification might lead to a solid phase with defects and amorphous fractions, so the density inside the nanotip could vary between 2.33 and 2.2 g/cm^3. Comparing calculated heights for monocrystal nanotip (Table I) and amorphous nanotip (Table II) with experimental tip's heights (Fig. 1), we see that though the calculated height are slightly lower, still the agreement with experiment is quite good for such a simplified model. The difference might be attributed to simplifications that were made, like the assumption β=const [instead of $\beta=\beta(R,z)$]. Also our model is quasistatic; there could be an additional hydrodynamic impact, namely, solidifying silicon creates an additional pressure in adjacent liquid silicon, producing a capillary wave which moves toward the center of the laser spot. Such a mechanism was considered in Ref. 21 to explain hillocks and ridges produced during amorphous thin film resolidification under the so called superlateral growth condition.

IV. COMPUTER SIMULATION

To prove our assumption about the predominantly lateral heat dissipation we provide numerical modeling of the heat transfer in a SOI structure subjected to a single pulse laser irradiation.

We performed a two-dimensional heat transfer and melting computer simulation in a system of two layers: thin 0.2 μm silicon film on silicon dioxide (SiO_2) substrate. The film was irradiated with a single 25 ns pulse of a fluence of 1.5 J/cm^2. Under these conditions melting starts during the first half of the pulse. Taking into account that at λ =248 nm the average reflectivity of hot solid Si is 63% and is 70% for liquid silicon,[22] we roughly have 0.45 J/cm^2 that can penetrate into the surface layer. Quite often the exact energy balance of light-matter interaction under the intense laser irradiation is not known. In the case of irradiation of 0.2 μm Si film with a considerably high fluence of 1.5 J/cm^2 we found that the vaporization ratio is not higher than several percent of the film material. Even that amount of ionized vapor can provide some shielding of laser irradiation that was not included in our calculations. We also assumed that at a higher fluence, a more significant amount of the absorbed energy can dissipate through nonthermal channels like electromagnetic radiation from the film, electron/ion emission, surface waves, and the stress energy being accumulated in film/substrate. Varying the part of the absorbed energy that can be converted to thermal energy we found that by assuming the thermal energy to be 0.22 J/cm^2 (i.e., about 50% of absorbed energy), we obtain a value for the maximum radius of melt that coincides with the experimentally observed melting spot of radius of about 2.5 μm. The heat transfer occurs in three dimensions but because of the axial symmetry it is formally two dimensional. The temperature field T is also time dependant, so in cylindrical coordinates we have $T=T(t,z,r)$. In our model silicon is treated as an incompressible substance, hence, enthalpy is equal to thermal energy per unit volume.

Let us consider a heat transfer equation for a silicon sample that contains two phases, liquid and solid[23]

$$\frac{\partial T}{\partial t} = \frac{Q(r,z,t)/\rho c + \sigma \Delta T}{1 + L_m \delta(T-T_m)/c}. \tag{10}$$

Here $Q(r,z,t)$ is a laser heat source, $\sigma=k/\rho c$ is the thermal diffusivity, k is the thermal conductivity, c is the specific heat, L_m is the latent heat of melting, r,z are cylindrical coordinates, and ρ is the density. The delta-function term in the equation reflects the latent heat absorbed or released at the phase transition temperature $T=T_m$ (Fig. 5). For computer simulation purposes the laser heat source was approximated by a homogeneous spot at the surface of silicon with a radius of 2.8 μm and a depth of 20 nm (while the absorption length for 248 nm radiation in Si is about 6 nm, the electron diffusion length evaluated for electron-lattice relaxation time 0.5 ps is of order of 15 nm); thermal conductivity and specific heat of Si were kept constant. The average thermal conductivity for solid silicon $\langle k \rangle \approx 0.5$ W/cm K, T_m=1685 K, the latent heat L_m=1650 J/g, the specific heat of solid Si at

TABLE I. Heights of monocrystalline cone for 0.2 μm silicon film, radius of irradiated spot R_o=2.8 μm, and different values of angle β according to expressions (6) and (7).

Angle β (deg)	R_{cr} (μm)	H_{cr} (μm)	$H(0)$ (μm)
2.5	0.019346	0.446340	0.478538
5	0.035222	0.402584	0.434791
10	0.064446	0.365490	0.394729
15	0.092440	0.344991	0.372591

TABLE II. Heights of amorphous cone for 0.2 μm silicon film, radius of irradiated spot R_o=2.8 μm and different values of angle β according to expressions (6) and (7).

Angle β (deg)	R_{cr} (μm)	H_{cr} (μm)	$H(0)$ (μm)
1.5	0.018169	0.693843	0.777104
2.5	0.027440	0.656242	0.703893
5	0.048064	0.549369	0.615293
10	0.084581	0.479683	0.537245

Downloaded 21 Oct 2008 to 128.205.254.133. Redistribution subject to AIP license or copyright; see http://jap.aip.org/jap/copyright.jsp

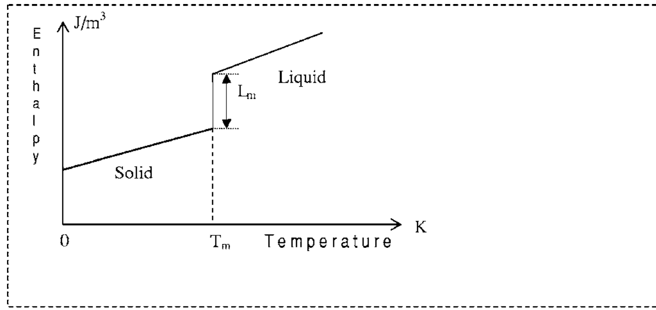

FIG. 5. Temperature dependence of enthalpy near solid-melt phase transition.

melting point $c=1.032$ J/(g K),[24] while it is 1.02 J/(g K) for liquid Si.[25] Introducing nondimensional variables in cylindrical coordinates, $T \to T/T_m$, $r \to r/R_0$, $z \to z/R_0$, $t \to t/t_0$, constants R_0 and t_0 were chosen to have the coefficient in front of Laplace operator, $k/(\rho \cdot c) \times t_0/R_0^2 \approx 1$.

The delta function in Eq. (10) was approximated by the finite function $\exp[-(T-1)^2/2\delta^2]/\sqrt{2\pi}\delta$,[23,26] where $\delta = 0.0297$ (which corresponds to 50 K temperature interval of phase transition around T_m). Then in Si we have

$$\frac{\partial T}{\partial t} = \frac{\Delta T k t_0/\rho c (R_0)^2 + Q t_0/\rho c T_m}{1 + 13.17 \exp[0.5(T-1)^2/\delta^2]} = \frac{\Delta T + Q_n}{1 + 13.17 \exp[0.5(T-1)^2/\delta^2]}, \tag{11}$$

where $\Delta T = \partial^2 T/\partial r^2 + 1/r \times \partial T/\partial r + \partial^2 T/\partial Z^2$; Q_n is a nondimensional heat source. Since the earlier equation describes solid/liquid phase transition, there is a discontinuity in the density ρ and in the thermal conductivity k on the phase border inside Si. In the case of constant k considered here, we use the value 0.57 W/cm K for liquid Si (Ref. 27) and the average (over the interval of 300°–1600°) value of k for solid Si, equal to 0.5 W/cm K. At the same time the density ρ changes from 2.32 to 2.52 g/cm^3, as a result the ratio $k/(\rho c)$ has quite a small discontinuity that could be neglected. Discontinuity in the term $Q/(\rho c)$ was also neglected at this stage, because this part of the equation is nonzero only during the first 25 s and the goal of the calculation was to determine how the frozen/melt border moves after the pulse. Some softening of the underlying silica substrate material is possible. However, in this model we choose to neglect any effects due to such softening and we treat the substrate as a solid. The thermal conductivity of fused silica, $k = 0.014$ W/cm K, is significantly lower than the thermal conductivity of silicon, and grows very slightly with temperature. So in the SiO_2 substrate

$$\partial T/\partial t = \Delta T \times 0.03. \tag{12}$$

The set of Eqs. (11) and (12) was solved numerically in two layers applying explicit forward time centered space finite difference schema. In order to make a time step, a subroutine for two-dimensional matrices introduced in Ref. 28 was used, $u_1 = \text{matrix}(0,n,0,m)$ and $u_2 = \text{matrix}(0,n,0,m)$ for the previous and the next time moments correspondingly. Zeros in matrices designate starting indices and will be omitted below. Since the matrix size is $n \times m$, for discrete coordinates in radial and vertical z direction we have $0 \le ir \le n$ and $0 \le iz \le m$. In terms of matrices we have $T(it, ir, iz) \to u_1(ir, iz)$; $T(it+1, ir, iz) \to u_2(ir, iz)$.

The initial condition for nondimensional temperature is $T(0,z,r) = 300K/T_m$.

The boundary conditions: on Si/SiO_2 interface ($iz = zb$ is the interface coordinate) we use the heat flux continuity condition: $k_{Si} \nabla T_{Si} = K_{SiO_2} \nabla T_{SiO_2}$ for any ir coordinate. It translates into a condition in terms of matrices

$$u_2(ir,zb) = [0.03 \times u_2(ir,zb+1) + u_2(ir,zb-1)]/1.03. \tag{13}$$

At the film surface $Z=0$ ($iz=0$) we neglected thermal conductivity of air:

$$\partial T(r,0)/\partial Z = 0;$$

it translates into a condition for matrices

$$u_1(ir,0) = u_1(ir,1). \tag{14}$$

Axial symmetry condition: At $r=0: \partial T(0,Z)/\partial r = 0$; at $r = 25: \partial T(0,r)/\partial r = 0$ (constant temperature far from the spot); it translates into a condition for matrices

$$u_1(0,iz) = u_1(1,iz); \quad u_1(n-1,iz) = u_1(n-2,iz). \tag{15}$$

After each time step, new temperature values on the Si/SiO_2 interface were found from the boundary condition (13) and other boundary conditions were applied. After obtaining $n \times m$ matrixes of temperature field for different time moments one can extract the position of $T = T_{melt}(r,z,t)$. Isothermal curves $T = T_{melt}$ in Si film at different time moments during the laser processing with a fluence 1.5 J/cm^2 are sown in Figs 6(a) and 6(b). The upper diagram in Fig. 6(a) represents melting for a laser spot radius 2.8 μm, $t < 25$ ns and the lower one is for resolidification. The resolidification process laser spot radius 1.7 μm is shown on Fig. 6(b) [the melting process is very similar to the one on Fig. 6(a) and is not shown].

V. DISCUSSION

As we can see from Fig. 6, during the laser pulse the melting front moves from the top to the bottom of the film, while the freezing front moves almost vertically from the edges toward the center, but eventually another freezing front emerges near to the substrate's surface. The average speed of lateral resolidification does not exceed 20 m/s. The length of lateral regrowth could be estimated as 1.5 μm. Comparing resolidification for spot radiuses 2.8 μm [Fig. 6(a)] and 1.7 μm [Fig. 6(b)], one can see that in case (a) the second front emerges at the bottom while the radius of melt at the top is about 800 nm [that resolidification process produces nanotip shown on Fig. 1(a)]. In case (b) the lateral resolidification continues until the radius of melt is about 150 nm, which leads to a sharper nanotip [see Fig. 1(b)].

Since the vertical elevation that we observe experimentally was not yet included in the simulation, it was possible to demonstrate only "sharper spike preconditions" like the predominantly lateral movement (toward the center) of the vertical phase border during the resolidification. Since the

Downloaded 21 Oct 2008 to 128.205.254.133. Redistribution subject to AIP license or copyright; see http://jap.aip.org/jap/copyright.jsp

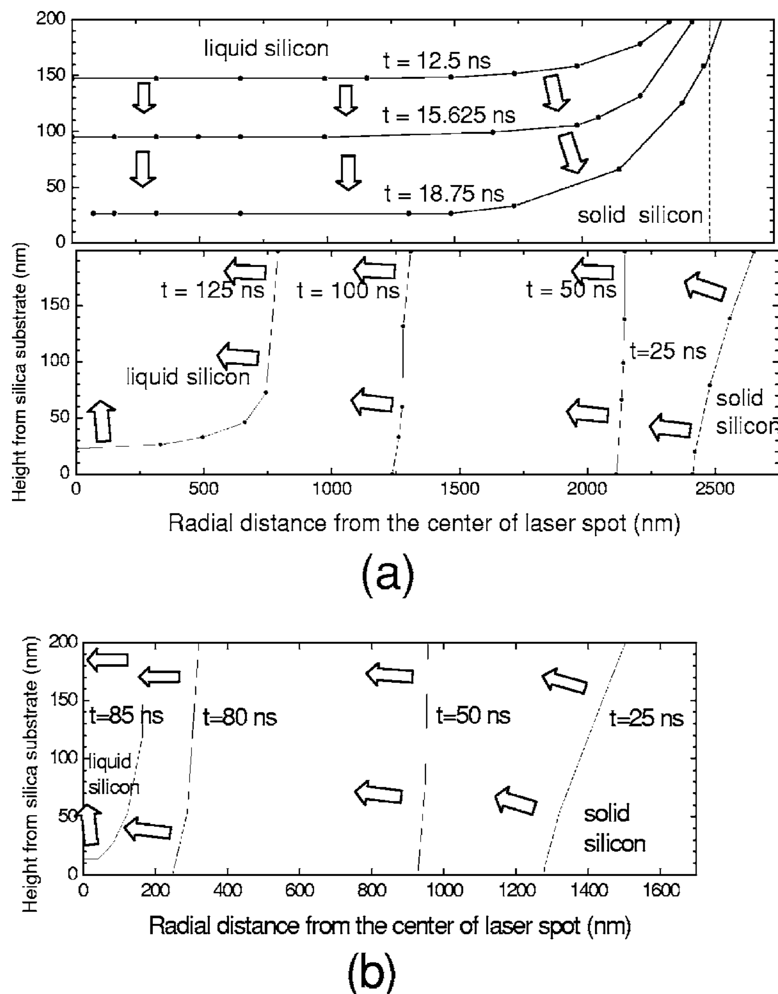

FIG. 6. Isotherms $T=T_m$ in Si film on SiO_2 substrate calculated at different time moments for the laser spot radius (a) 2.8 and (b) 1.7 μm. Arrows show the direction of liquid silicon movement.

heat dissipation from elevated areas becomes more difficult, the areas near the surface stay overheated, so in elevated layers the phase border will be probably more pronounced for a longer period of time, while silicon layers near the substrate would be already frozen.

Although the simulation with a fixed film thickness cannot provide adequate details near $r=0$ at the very end of resolidification, overall it gave us important insights and data in support of our analytical model. The ratio $\overline{\partial T/\partial r}|_{r=R_0}/\overline{\partial T/\partial z}|_{z=z_b}$ obtained from the computer simulation at the time of 50 ns (corresponds to a quite perfect lateral resolidification phase, see Fig. 6) is about 8.4, hence, according to criterion (1), for 200 nm films the condition $R_{\rm spot} < 3.5$ μm should be fulfilled for a laser spot.

Indeed, when a larger, 100 μm diameter pinhole mask was used ($R_{\rm spot}=5.6$ μm), no cones were formed.

When the thickness of the film was increased while still using the 50 μm pinhole mask (i.e., $R_{\rm spot}=2.8$ μm), there were no observable changes on the surfaces of the films with thicknesses of 2.3 and 4.1 μm after single-pulse irradiation with fluences up to 3.0 J/cm^2. In this case the condition for film thickness $H_{\rm film} < \sqrt{\sigma\tau} < R_{\rm spot}$ was violated.

It is useful to compare our results with results reported in Ref. 20 for bulk silicon, where dimple-shaped features with diameters 1–4 μm and depths 1–300 nm were produced on bulk Si wafers by varying the laser-spot diameter and the peak energy densities in the range of 0.4–1.3 J/cm^2: similar to our experiment, a single one nanosecond pulse was concentrated on the silicon surface spot with a diameter of about 3 μm. The authors of Ref. 20 explain surface nanostructuring by a two-dimensional fluid-flow driven by gradients in the surface tension of molten silicon. Since we used spatially homogenized, 25 ns pulses and bigger spot sizes, our radial temperature gradients were smaller in comparison with Ref. 20. The excimer laser beam spatial profile in our case was closer to a trapezoidal one rather than to a Gaussian profile used in Ref. 20. As a result, temperature gradients were created predominantly at the edges of the irradiated spot. That might explain why we did not observe a noticeable vertical profile on bulk silicon.

The authors of Ref. 20 also presented data that were obtained using a different, frequency doubled Nd:YLF laser, with a longer, 15 ns pulse and a laser spot of 8 μm in diameter (quite close to our parameters). In this case their peak to peak roughness exceeded 100 nm only for fluences larger that 2 J/cm^2. At the highest fluence that we used, 2 and 2.5 J/cm^2, we observed a deep hollow inside the cone (see Fig. 7). For these fluences the vertical profile created in the film at resolidification time looked like a superposition of a cone and the dimple-shaped vertical profile observed in Ref. 20.

Downloaded 21 Oct 2008 to 128.205.254.133. Redistribution subject to AIP license or copyright; see http://jap.aip.org/jap/copyright.jsp

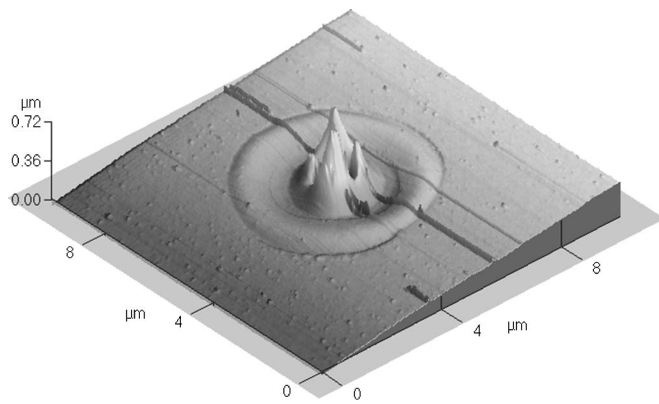

FIG. 7. AFM image of nanostructure fabricated by a single pulse with fluence of 2.5 J/cm^2 and the laser spot radius of 2.8 μm.

VI. CONCLUSIONS

Computer simulations confirmed that resolidification occurs predominately laterally with a phase border moving toward the center of the laser spot. The calculated lateral growth length of order of 1.5 μm is in agreement with experimentally measured lateral growth lengths in silicon films after laser irradiation.[29] We showed that in the particular case of silicon film the difference in liquid/solid densities under condition of lateral resolidification will lead to cone formation. Experimental results are consistent with the introduced lateral heat flow criterion (1). Further experimental efforts are needed to determine the crystalline state of the material comprising the Si nanotip.

We have also shown that a multidimensional computer simulation like the one described earlier can serve to optimize experimental parameters and fabricate desirable Si micro-/nanostructures.

[1]L. Dvorson, I. Kymissis, and A. I. Akinwande, J. Vac. Sci. Technol. B **21**, 486 (2003).
[2]H. H. Busta, J. Micromech. Microeng. **2**, 43 (1992).
[3]S. Turner, L. Kam, M. Isaacson, H. G. Craighead, W. Shain, and J. Turner, J. Vac. Sci. Technol. B **15**, 2848 (1997).
[4]A. M. P. Turner, N. Dowel, S. W. P. Turner, L. Kam, M. Isaacson, J. N. Turner, H. G. Craighead, and W. Shain, J. Biomed. Mater. Res. **51**, 430 (2000).
[5]M. P. Maher, J. Pine, J. Wright, and Y. C. Tai, J. Neurosci. Methods **87**, 45 (1999).
[6]A. J. Pedraza, J. D. Fowlkes, and D. H. Lowndes, Appl. Phys. Lett. **74**, 2322 (1999).
[7]A. J. Pedraza, J. D. Fowlkes, and Y. F. Guan, Appl. Phys. A: Mater. Sci. Process. **77**, 277 (2003).
[8]C. Wu *et al.*, Appl. Phys. Lett. **78**, 1850 (2001).
[9]S. Juodkazis, H. Misawa, O. Louchev, and K. Kitamura, Nanotechnology **17**, 4802 (2006).
[10]S. M. Huang, Z. Sun, B. S. Luk'yanchuk, M. H. Hong, and L. P. Shi, Appl. Phys. Lett. **86**, 161911 (2005).
[11]G. Wysocki, R. Denk, K. Piglmayer, N. Arnold, and D. Bäuerle, Appl. Phys. Lett. **82**, 692 (2003).
[12]D. G. Georgiev, R. J. Baird, I. Avrutsky, G. Auner, and G. Newaz, Appl. Phys. Lett. **84**, 4881 (2004).
[13]D. G. Georgiev, R. J. Baird, I. Avrutsky, J. Eizenkop, G. Auner, and G. Newaz, Spring Meeting of the Materials Research Society, San Francisco, CA, April 2006, Symp. L, p. 252, http://www.mrs.org.
[14]S. de Unamino and E. Fogarassy, Appl. Surf. Sci. **36**, 1 (1989).
[15]I. Avrutsky, D. G. Georgiev, D. Frankstein, G. Auner, and G. Newaz, Appl. Phys. Lett. **84**, 2391 (2004).
[16]I. A. Avrutskii, P. V. Bazakutsa, A. M. Prokhorov, and V. A. Sychugov, Sov. Tech. Phys. Lett. **11**, 258 (1985).
[17]A. M. Prokhorov, I. A. Avrutsky, P. V. Bazakutsa, V. A. Sychugov, and A. V. Tischenko, in *Nonlinear Surface Electromagnetic Phenomena*, edited by H.-E. Ponath and G. I. Stegeman (Elsevier Science, Amsterdam, 1991), p. 525.
[18]D. G Georgiev, R. J. Baird, I. Avrutsky, G. Auner, G. Newaz, and N. Torkanova, Mater. Res. Soc. Symp. Proc. **872**, J.13.6 (2005).
[19]T. Chiba, R. Komura, and A. Mori, Jpn. J. Appl. Phys., Part 1 **39**, 4803 (2000).
[20]T. Schwarz-Selinger, D. G. Cahill, S.-C. Chen, S.-J. Moon, and C. P. Grigoropoulos, Phys. Rev. B **64**, 155323 (2001).
[21]D. K. Fork, G. B. Anderson, J. B. Boyce, R. I. Johnson, and P. Mei, Appl. Phys. Lett. **68**, 2138 (1996).
[22]G. E. Jellison, D. H. Lowndes, D. N. Mashburn, and R. F. Wood, Phys. Rev. B **34**, 2407 (1986).
[23]V. A. Pilipovich, V. L. Malevich, G. D. Ivlev, and V. V. Zhidkov, J. Eng. Phys. **48**, 228 (1985).
[24]R. Hull, *Properties of Crystalline Silicon* (The Institution of Electrical Engineers, Stevenage, UK, 1999), Chap. 4.1.
[25]H. Nagai *et al.*, Jpn. J. Appl. Phys., Part 1 **39**, 1405 (2000).
[26]N. M. Bulgakova, A. V. Bulgakov, and L. P. Babich, Appl. Phys. A: Mater. Sci. Process. **79**, 1323 (2004).
[27]E. Yamasue, M. Susa, M. Hayashi, H. Fukuyama, and K. Nagata, Book of Abstracts of the 15th European Conference of Thermophysical Properties, Wurzburg, Germany, September 1999.
[28]W. H. Press, B. P. Flannery, S. A. Teukolsky, and W. T. Vetterling, *Numerical Recipes in C*, 2nd ed. (Cambridge University Press, New York, 1997), p. 20.
[29]H. Kisdarjono, A. Voutsas, and R. Solanki, J. Appl. Phys. **94**, 4374 (2003).

Downloaded 21 Oct 2008 to 128.205.254.133. Redistribution subject to AIP license or copyright; see http://jap.aip.org/jap/copyright.jsp